Phonon-assisted transport through a single quantum dot with impurity scattering effects

2004 J. Phys.: Condens. Matter 16 8285

(http://iopscience.iop.org/0953-8984/16/46/015)

INSTITUTE OF PHYSICS PUBLISHING JOURNAL OF PHYSICS: CONDENSED MATTER

J. Phys.: Condens. Matter **16** (2004) 8285–8295 PII: S0953-8984(04)81225-6

Phonon-assisted transport through a single quantum dot with impurity scattering effects

B H Wu and J C Cao

State Key Laboratory of Functional Materials for Informatics, Shanghai Institute of Microsystem and Information Technology, Chinese Academy of Sciences, 865 Changning Road, Shanghai 200050, People's Republic of China

E-mail: bhwu@mail.sim.ac.cn

Received 25 May 2004, in final form 2 August 2004
Published 5 November 2004
Online at stacks.iop.org/JPhysCM/16/8285
doi:10.1088/0953-8984/16/46/015

Abstract

In this paper, we calculate the current and shot noise for electrons transporting through a single quantum dot with phonon and impurity scatterings. By iteratively calculating the surface Green function, we obtain the self-energy due to coupling between the quantum dot and the semi-infinite leads. Significant couplings to the localized phonon modes and impurity states are included in our model exactly. Our results show that the resonance transmission coefficient and differential conductance split into small peaks in the presence of dot–impurity interaction. Satellite peaks caused by phonon emission (absorption) appear in our results too. As the numerical results, impurity states have weak influence on the suppression of shot noise. On the other hand, shot noise in the conductor will be enhanced if the phonon mode effects are included in our calculations.

1. Introduction

With advanced microfabrication and self-assembly techniques, it is now possible to explore the transport properties of quantum dots and molecular electronics. The quantum nature of these devices has attracted much attention and a lot of potential applications have been proposed. For example, large on–off ratios and negative differential resistance in a molecular electronic device have been experimentally obtained [1] and theoretically studied [2]. Coherent superposition of photon- and phonon-assisted tunnelling in coupled quantum dots has been experimentally observed [3] too. Recently, the Kondo effect in a quantum dot molecule coupled with an Anderson impurity has been theoretically investigated using the infinite-U slave-boson mean-field approximation [4]. It is found that the single-channel conductance can be completely suppressed by Kondo scattering. The effects of interdot Coulomb interaction on the transport properties of a double-quantum-dot structure have been investigated by a Green function approach [5]. Numerical results show that the interdot interaction can produce

a significant change in the transport properties of this coupled quantum dot system even if it is much weaker than the on-dot Coulomb interaction. These achievements motivate the rapidly growing research on quantum dot and molecular electronic devices. Current research uses molecules and quantum dots in such electronics applications as interconnects, switches, rectifiers, transistors, nonlinear components, photovoltaics, and memories [6, 7]. However, the considerable dephasing induced by various scatterings imposes a limit to these potential applications. The investigation of dissipation processes in these nanostructures is thus of great significance. But it is nontrivial to treat these interactions with a fully quantum mechanical concept. Different methods such as the Green function method, the master equation approach, and the bosonization technique have been developed to handle this problem. In the scattering approach, the current through an elastic molecular wire junction can be viewed as charge carrier transmission and expressed as the well known Landauer formula [8]. But this formula does not include the inelastic scattering effects caused by interaction. Hence a generalized Landauer formula for current through a region of interacting electrons is derived by the nonequilibrium Keldysh formula [9].

Recently, theoretical and experimental research on shot noise in small conductors has attracted much attention [10–17]. Current noise is caused by the time-dependent fluctuation. It is interesting that noise in mesoscopic structures can reveal the kinetics of electrons [16]. Information which cannot be obtained by measuring the conductance can be obtained from the measurement of the noise characteristics of a conductor. At nonzero temperature, both thermal noise and shot noise are two fundamental noise sources. The thermal noise caused by thermal fluctuations is related to the conductance of the system. The shot noise is a direct consequence of the discrete nature of the charge transport when the system is out of equilibrium. In the past years, most of the theoretical studies on shot noise in mesoscopic systems have concentrated on noninteracting electrons. However, scattering effects in the quantum dots have shown profound influences on the noise spectra of mesoscopic conductors. For example, both suppression [18–20] and enhancement [13, 21] of shot noise from the Poisson value of shot noise $2eI$ due to Coulomb interaction have been observed by several experiments. Gurvitz *et al* systematically studied the current and shot noise of mesoscopic devices interacting with environment or detectors by using the Bloch-type rate equations [10, 11, 22]. By employing a finite-U slave-boson mean-field approach, Dong *et al* numerically investigated the suppression of shot noise due to the Kondo-correlation effect [23]. Recently, effects of the phonon–electron coupling on the current and shot noise behaviour of the quantum dot devices have been studied by using the nonequilibrium Keldysh formula [14]. It has been experimentally found that the presence of the impurity states in low dimensional nanostructures plays an important role in the transport and optical properties [17, 24, 25]. For example, noise caused by capture and emission of one electron by a single trap state was recently studied experimentally and theoretically [17].

The purpose of this paper is to focus on the superposition of the impurity states and phonon modes effects on the transport properties of a single quantum dot device coupled with two semi-infinite leads. In contrast to the strong Coulomb repulsion case, we will focus on the opposite limit where the quantum dot electron can interact with phonon modes and the impurity states while the electron–electron interaction in the impurity can be ignored. We calculate the current and shot noise of a single molecular quantum dot interacting with impurity states and localized phonon modes. All the other interactions in the molecular devices are neglected. In order to simplify our discussions, the coupling between the dots and the leads is assumed to be small and only the quantum dot electrons can interact with the impurity states and phonon mode. Thus we can neglect the coupling between the phonon mode and impurity states with the leads.

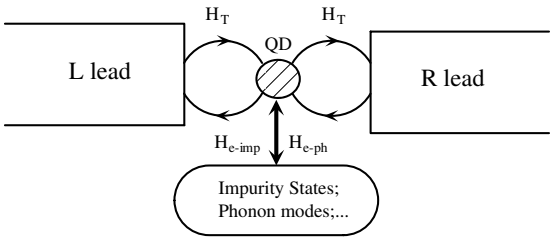

Figure 1. Transport through a molecular quantum dot system with one level. Electrons in the left (L) and right (R) leads can hop onto/off the quantum dot. The quantum dot can interact with the impurity states and the phonon modes existing in this system.

2. Theoretical model

We consider a tight binding model Hamiltonian and neglect any effects of electron–electron interaction. The system we study consists of a semi-infinite left lead, a central part and a semi-infinite right lead. A schematic diagram of this mesoscopic device is shown in figure 1. The degrees of freedom of the central part are characterized by two coupled sets of states. One is the quantum dot which is coupled with the lead via tunnelling. The other is the impurity state. Electron hopping in the quantum dot, from the leads, can either hop forward or back to the leads or to the impurity due to internal scattering. Electrons in the impurity state can hop back to the quantum dot too. Here we assume the impurity states to be isolated and noncorrelated. Only a single impurity state f exists in the system. Interaction between the electrons and the phonon mode localized on the dot is also included in our model. Quantum dot phonons play an important role in the optical and electrical properties of quantum dots. The phonon effects are taken into consideration by the Einstein model, where all the phonons have the same energy ω_0 ($\hbar = 1$). This simplest single-phonon mode is used to address the phonon effects in the semiconductor quantum dot due to spatial confinement [26, 27] or the vibrational degrees of freedom in the molecular dot [14].

The total Hamiltonian is given by

$$H = H_{\mathrm{L}} + H_{\mathrm{R}} + H_{\mathrm{C}} + H_{\mathrm{T}} + H_{\mathrm{ph}} + H_{\mathrm{imp}} + H_{\mathrm{e-ph}} + H_{\mathrm{e-imp}} \tag{1}$$

where the term

$$H_{\mathrm{L}} + H_{\mathrm{R}} = \sum_{i \neq 0,-1} t(c_i^{\dagger} c_{i+1} + \mathrm{h.c.}) \tag{2}$$

describes the left and the right leads. Only the nearest neighbour interactions are important. The hopping matrix element on the two leads is t. c_i ($c_i^{\dagger}$) is the annihilation (creation) operator acting on site i.

The term H_{C} in equation (1) describes the noninteracting quantum dot and has the following form:

$$H_{\mathrm{C}} = \epsilon_0 d^{\dagger} d, \tag{3}$$

where ϵ_0 denotes the energy of the discrete dot level. There should be many discrete energy levels in a quantum dot. In our case, we take only one energy level into account for simplicity. This simplicity is valid for systems with resonant level such as a molecule or single-level quantum dot. In these systems, the contribution by the other dot states can be ignored [27].

The phonon modes and the isolated impurity states Hamiltonian are given by

$$H_{\mathrm{ph}} = \omega_0 a^{\dagger} a, \tag{4}$$

$$H_{\mathrm{imp}} = f b^{\dagger} b, \tag{5}$$

respectively.

The other terms $H_{\rm T}$, $H_{\rm e-ph}$ and $H_{\rm e-imp}$ describe the tunnelling processes between the dot and the electrodes, the interaction between the dot and the phonon mode and the interaction between the dot and the impurity state respectively. These terms take the form

$$H_{\rm T} = v(d^\dagger c_1 + d^\dagger c_{-1} + \text{h.c.}), \tag{6}$$

$$H_{\rm e-ph} = \lambda(a + a^\dagger)d^\dagger d, \tag{7}$$

$$H_{\rm e-imp} = s(b^\dagger d + \text{h.c.}), \tag{8}$$

where v is the component of the tunnelling matrix and represents the energy associated with hopping onto/off the dot, λ is the coupling constant between the dot electrons and the phonon mode and s is the coupling strength to the impurity state. Here we assume that the electron–phonon interaction is restricted to the quantum dot.

Following the standard procedures, we can diagonalize the Hamiltonian $H_0 = H_{\rm C} + H_{\rm ph} + H_{\rm e-ph}$ by making a canonical transformation [28, 14]. The transformation is $\bar{H}_0 = e^S H_0 e^{-S}$, where $S = d^\dagger d(\lambda/\omega_0)(a^\dagger - a)$. This canonical transformation gives

$$\bar{H}_0 = e^S H_0 e^{-S} = d^\dagger d(\epsilon_0 - \Delta) + \omega_0 a^\dagger a, \tag{9}$$

where $\Delta = \lambda^2/\omega_0$. It is straightforward to see

$$\bar{d} = dX; \qquad \bar{d}^\dagger = d^\dagger X^\dagger, \tag{10}$$

where the operator X is defined as

$$X = \exp[-\lambda/\omega_0(a^\dagger - a)]. \tag{11}$$

The dot–electron retarded (r) and advanced (a) Green function can then be written as

$$\begin{aligned} G^{\rm r(a)}(t) &= \mp {\rm i}\theta(\pm t)\langle\{\bar{d}(t), \bar{d}^\dagger(0)\}\rangle_{\rm e}\langle X(t)X^\dagger(0)\rangle_{\rm ph} \\ &= \bar{G}^{\rm r(a)}(t)\langle X(t)X^\dagger(0)\rangle_{\rm ph}. \end{aligned} \tag{12}$$

The factor $\langle X(t)X^\dagger(0)\rangle_{\rm ph}$ is due to the coupling to the phonon mode and can be written as

$$\langle X(t)X^\dagger(0)\rangle_{\rm ph} = {\rm e}^{-\Phi(t)}, \tag{13}$$

where

$$\Phi(t) = (\lambda/\omega_0)^2[N_{\rm ph}(1 - {\rm e}^{{\rm i}\omega_0 t}) + (N_{\rm ph} + 1)(1 - {\rm e}^{-{\rm i}\omega_0 t})]$$

and $N_{\rm ph}$ is the phonon number. Equation (13) can be expanded in a power series in $\exp({\rm i}\omega_0 t)$ at zero or finite temperature [28]. The Green function $\bar{G}^{\rm r(a)}$ can be obtained by the equation of motion method. From appendix A, the quantum dot Green function can be written as

$$\bar{G}^{\rm r}_{\rm Dot}(\omega) = \frac{\omega - f}{(\omega - (\epsilon_0 - \Delta) - \Sigma^{\rm r})(\omega - f) - s^2}, \tag{14}$$

where the retarded self-energy $\Sigma^{\rm r} = \Sigma^{\rm r}_{\rm L} + \Sigma^{\rm r}_{\rm R}$ is due to the tunnelling into the left and the right electrical leads. The leads are assumed to be unaffected by the localized phonon modes and impurity states. Calculation details of the Green function and the self-energy are presented in appendices A and B respectively. The Green function $G^{\rm r(a)}_{\rm Dot}$ can be solved by using equations (12)–(14).

If the electron–impurity and electron–phonon coupling is weak enough, the current through the quantum dots with phonon modes and impurity states can be given by the generalized Landauer formula [9]

$$I = \frac{2e}{h}\int {\rm d}\epsilon\,[f_{\rm L} - f_{\rm R}]T, \tag{15}$$

where $T = G^{\rm a}_{\rm Dot}\Gamma_{\rm L}G^{\rm r}_{\rm Dot}\Gamma_{\rm R}$ is the transmission coefficient and $\Gamma = {\rm i}(\Sigma^{\rm r} - \Sigma^{\rm a})$ is the level-width function. The prefactor 2 in equation (15) arises from the spin degeneracy. The level-width

function is commonly determined under the wide-band limit approximation. This limit reflects no feature of the two semi-infinite lead and loses much information on the coupling between the quantum dot and the leads. In our calculations, the self-energy is iteratively determined by the surface Green function instead of by simply using the wide-band limit. Details of the calculation are presented in appendix B. $f_{\rm L}(\epsilon) = f(\epsilon + eV/2)$ and $f_{\rm R}(\epsilon) = f(\epsilon - eV/2)$ are the Fermi distribution functions of the two leads when the quantum dot device is biased with the voltage V. Here, an assumption of a symmetric voltage drop through the whole system is made.

From equation (15) the differential conductance is found to be

$$C = \frac{{\rm d}I}{{\rm d}V} = \frac{e^2\beta}{h}\int {\rm d}\epsilon\,[f_{\rm L}(1-f_{\rm L}) + f_{\rm R}(1-f_{\rm R})]T, \tag{16}$$

where $\beta = 1/k_{\rm B}{\rm T}$, $k_{\rm B}$ is the Boltzmann constant and T is the temperature.

Due to the particle nature of the charge transport, shot noise in the two-terminal electrical conductor is the direct result of the time-dependent fluctuation of current. Due to current conservation, the correlation function of current is defined as [14, 15]

$$S(t,t') = S_{\rm L,L}(t,t') = \tfrac{1}{2}\langle\{\Delta\hat{I}_{\rm L}(t), \Delta\hat{I}_{\rm L}(t')\}\rangle, \tag{17}$$

where we have introduced the operator $\Delta\hat{I}_{\rm L}(t) = \hat{I}_{\rm L}(t) - \langle\hat{I}_{\rm L}(t)\rangle$ and $\{\cdots\}$ is the anticommutator. The Fourier transform of this correlation function $S(\omega)$ is always referred to as noise power. We will only be interested in zero-frequency limit noise $S(0)$. In the weak electron–phonon and electron–impurity coupling limit, the shot noise of the quantum dot system can be written in terms of transmission coefficient as [15]

$$S(0) = \frac{4e^2}{h}\int {\rm d}\epsilon\,\{[f_{\rm L}(1-f_{\rm L}) + f_{\rm R}(1-f_{\rm R})]T + (f_{\rm L}-f_{\rm R})^2(1-T)T\}. \tag{18}$$

Here the first term is the equilibrium noise contributions, and the second term is the nonequilibrium or shot noise contribution to the power spectrum.

3. Numerical results and discussion

In this section, the numerical results for the current and the noise are presented and discussed.

Current behaviour in a molecular quantum dot influenced by the coupled phonon mode has been studied in detail before [27, 28]. The absorption or emission of an n-phonon process shows a fundamental effect on the transport characteristics of the mesoscopic system. We will focus on the case where an impurity state and localized phonon mode in the central part are coexistent and can interact with the quantum dot simultaneously.

From equations (15) and (18), we can see that the transmission coefficient is the key parameter in determining the transport properties of the mesoscopic conductor. In figure 2, transmission coefficients with different quantum dot–impurity coupling strength s are plotted. The energy of the quantum dot level $\epsilon_0 = 5.0$ (in unit of $\hbar\omega_0$). The impurity states have the same energy level as the quantum dot. The quantum dot–phonon coupling strength is fixed at $\lambda = 0.4$. The temperature is $k_{\rm B}T = 1.5$. The maximum transmission coefficient is less than unity due to the electron–phonon interaction at finite temperature. When $s = 0$, the quantum dot does not interact with the impurity state. Only the phonon modes are taken into account. We can see that the resonance has shifted by Δ to the left due to electron–phonon interaction. Small resonant shoulders at the right and left of the main resonant peak are due to the absorption and emission of phonons. The separation between these peaks is just the frequency of the phonon mode. When the impurity states are included in the

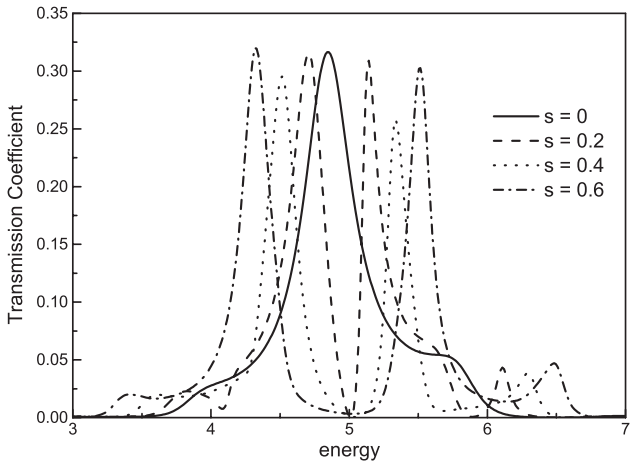

Figure 2. Transmission coefficient as a function of the energy at different dot–impurity coupling strengths. Solid curve, $s = 0$; dashed curve, $s = 0.2$; dotted curve, $s = 0.4$; dot–dashed curve, $s = 0.6$. Here, $\lambda = 0.4$, $f = 5.0$ and $k_B T = 1.5$.

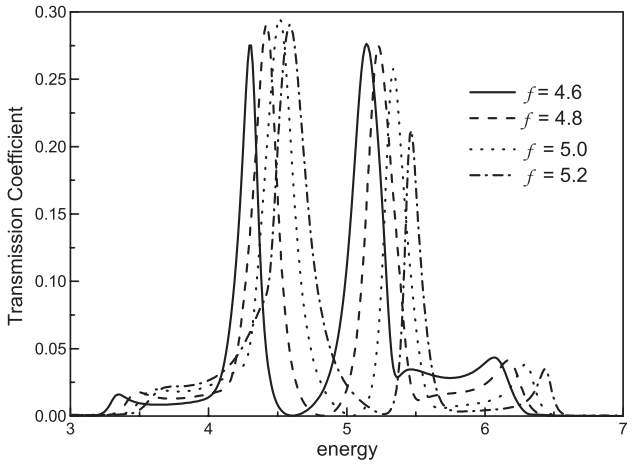

Figure 3. Transmission coefficient as a function of the energy at different impurity state energy levels. Solid curve, $f = 4.6$; dashed curve, $f = 4.8$; dotted curve, $f = 5.0$; dot–dashed curve, $f = 5.2$. Here, $\lambda = s = 0.4$ is fixed and $k_B T = 1.5$.

calculation ($s \neq 0$), the transmission coefficient resonant peak will be split into two peaks. The transmission coefficient at the impurity state energy will be zero. Small resonant peaks due to dot electron–phonon interaction are clearly shown in this figure even in the presence of impurity states. The splitting of the main resonant peak can be explained as follows. The central part energy levels are not only determined by the quantum dot when impurity states exist. The eigenstates of the central part are the combination of the quantum dot level and the impurity state energy. This is analogous to the formation of a two-atom molecule. The separation between the two final energy levels is relative to the coupling strength between these two states. The separation between the two split peaks increases with the coupling strength. Zero transmission coefficient at the impurity state energy can be directly seen from equation (14), where the Green function at $\omega = f$ is zero in the presence of dot–impurity interaction. Since the resonance energy of the central part is not only determined by the dot energy but also by the impurity level, the transmission coefficient is expected to be sensitive to the location of the impurity states. In figure 3, transmission coefficients are presented at different impurity state energies. The quantum dot–phonon coupling strength is fixed at $\lambda = 0.4$ and the coupling between the quantum dot and the impurity state is set to be $s = 0.4$. The quantum dot energy is set to be 5. When the impurity state energy f varies from 4.6 to 5.2,

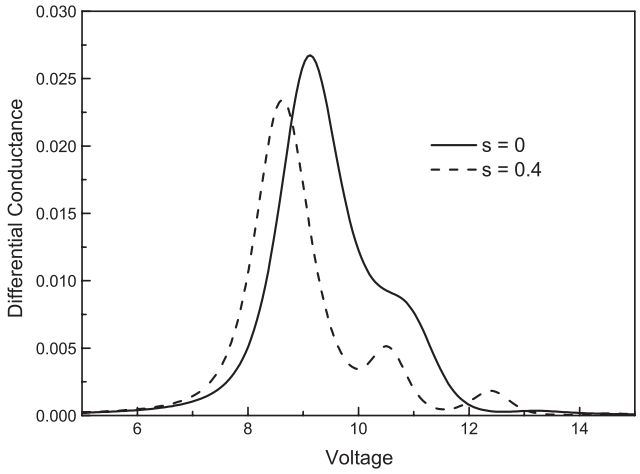

Figure 4. Differential conductance versus voltage at different dot–impurity coupling strengths in the presence of dot electron–phonon interaction. Solid curve, $s = 0$; dashed curve, $s = 0.4$. Here, $\lambda = 0.7$ and $f = 5.0$.

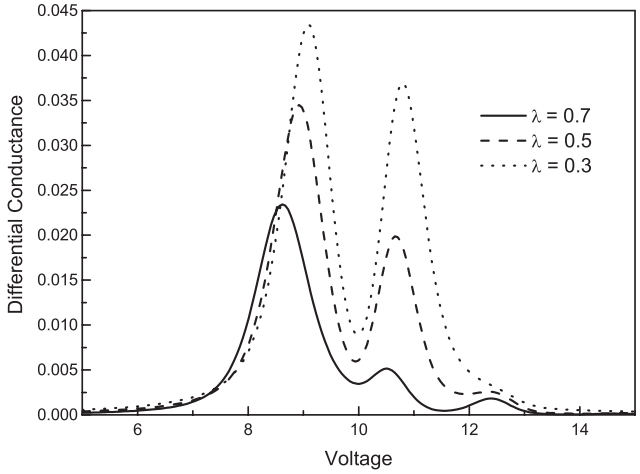

Figure 5. Differential conductance versus voltage at different electron–phonon coupling strengths in the presence of dot–impurity interaction. Solid curve, $\lambda = 0.7$; dashed curve, $\lambda = 0.5$; dotted curve, $\lambda = 0.3$. Here, $s = 0.4$ and $f = 5.0$.

the transmission resonance energy shifted to a higher value. This indicates that by changing the relative places of the impurity state and the quantum dot energy level, the resonant energies can be tuned.

Figures 4 and 5 depict the differential conductance using equation (16) with different coupling strengths. In figure 4, quantum dot–phonon coupling strength is fixed at $\lambda = 0.7$. The differential conductance is calculated in the presence ($s = 0.4$) and absence ($s = 0$) of dot–impurity state interaction. We can see that the differential conductance is sensitive to the existence of interaction between the dot and the impurity states. If there is no impurity state effect ($s = 0$), a shoulder to the right of the resonant energy appears in the plot due to strong electron–phonon coupling. The temperature in our calculation is low ($k_{\mathrm{B}}T = 0.1$). There are no available phonons to absorb and only the emission processes contribute to the transport behaviour. Thus, no satellite peaks at the left of the resonant peak are observed. In the presence of quantum dot–impurity state interaction ($s = 0.4$), the peak of the differential conductance shifts to the left. This is in accordance with figure 2, where the transmission coefficient splits due to quantum dot–impurity coupling. The first transmission coefficient peak appears to the left of the original resonance peak. In figure 5, we calculate the differential conductance with different electron–phonon coupling strengths. In our calculations, electron–impurity coupling

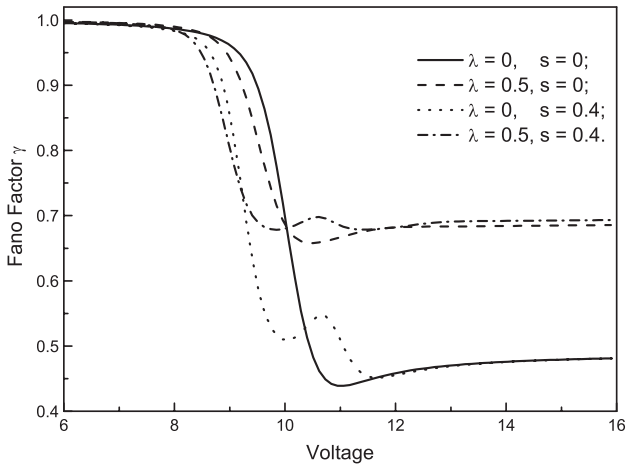

Figure 6. The Fano factor versus the voltage. Solid curve, $\lambda = s = 0$; dashed curve, $\lambda = 0.5, s = 0$; dotted curve, $\lambda = 0, s = 0.4$; dot–dashed curve, $\lambda = 0.5, s = 0.4$.

strength ($s = 0.4$) and the temperature ($k_{\mathrm{B}}T = 0.1$) are fixed. The differential conductance will show two peaks in the presence of impurity states. But these peaks can be reduced by the phonon effects. From figure 5, we can see that the differential conductance amplitude decreases with the increase of λ. At the same time, the second peak shows a much greater reduction in the coexistence of impurity states and phonon mode scatterings.

Different scattering effects on the shot noise power spectrum can be conveniently characterized by the Fano factor which is defined as the ratio of the shot noise and the full Poisson value. The Fano factor γ can be written as

$$\gamma = \frac{S(0)}{2eI}. \tag{19}$$

The Fano factor is a useful quantity to characterize the suppression of the shot noise from the full Poisson value. In figure 6, we depict the Fano factor as a function of the applied voltage at four different sets of electron–phonon and dot–impurity coupling strength parameters. When the applied voltage is small, the Fano factor is nearly unity. But when electrons in the lead can resonantly transport though the quantum dot with the increase of the applied voltage, the Fano factor will be suppressed. From figure 6, we can see that the resonance energy is shifted to the lower energy side when the dot–impurity interaction is turned on. This can be explained by the resonance transmission coefficient splitting due to dot–impurity interaction depicted in figure 2. When there is no electron–phonon interaction ($\lambda = 0$) and the applied voltage is large, the Fano factor will approach the well known limit $\gamma = 0.5$. The minimum Fano factor value appears near the resonance. If the electron–phonon interaction is turned on ($\lambda = 0.5$), the Fano factor is much larger than that in the absence of the electron–phonon interaction ($\lambda = 0$) no matter whether the dot–impurity interaction is turned on or not. This is due to the weaker resonant transmission coefficient when the quantum dot can strongly interact with the localized phonon modes. The electron–phonon interaction is dominant in determining the shot noise spectra. This suggests a more efficient noise reduction for conductors with a weaker electron–phonon interaction.

4. Conclusions

Using the generalized Landauer formula, we have numerically studied the current and shot noise of a single quantum dot coupled to both the impurity states and the phonon modes.

Satellite peaks appear due to the electron–phonon interaction. The presence of impurity states will split the resonant peak associated with the quantum dot energy level. By tuning the impurity state energy or the dot–impurity coupling strength, the splitting can be adjusted. This can be experimentally achieved by applying a gate probe to the single quantum dot. When the probe is close to the quantum dot, they can interact with each other. By tuning the interaction strength of the probe and the quantum dot, changes of the splitting of the resonant peak might be experimentally observed.

Acknowledgments

This work was supported by the Key National Science Foundation of China, the Special Funds for Major State Basic Research Project (G20000683 and 2001CCA02800), and the Special Funds for Shanghai Optic Engineering (011661075).

Appendix A. Green function of the central part

If a quantum dot is coupled to the left and right semi-infinite lead, we can divide the system into three parts: the central part (C), the left lead (L) and the right lead (R). The Green function can be expressed as

$$G = (\omega - H)^{-1} = \begin{pmatrix} \omega - H_{\mathrm{L}} & -H_{\mathrm{LC}} & 0 \\ -H_{\mathrm{CL}} & \omega - H_{\mathrm{C}} & -H_{\mathrm{CR}} \\ 0 & -H_{\mathrm{RC}} & \omega - H_{\mathrm{R}} \end{pmatrix}^{-1}. \tag{A.1}$$

The central part Green function can then be written as

$$G_{\mathrm{C}} = (\omega - H_{\mathrm{C}} - \Sigma_{\mathrm{R}} - \Sigma_{\mathrm{L}})^{-1}, \tag{A.2}$$

where $\Sigma_{\mathrm{L(R)}} = H_{\mathrm{CL(R)}} G_{\mathrm{L(R)}} H_{\mathrm{L(R)C}}$ is the self-energy due to the coupling between the central part and the two leads.

If an impurity state exists in the central part and this impurity state can interact with the quantum dots, the Hamiltonian is given by

$$H = H_{\mathrm{L}} + H_{\mathrm{R}} + H_{\mathrm{T}} + H_{\mathrm{C}} + H_{\mathrm{imp}} + H_{\mathrm{e-imp}}, \tag{A.3}$$

where H_{L}, H_{R}, H_{C}, H_{T}, H_{imp} and $H_{\mathrm{e-imp}}$ are given in equations (2), (3), (5), (6) and (8).

The Green function for the central part consisting of the quantum dots and the impurity states is then written in the matrix form as

$$G_{\mathrm{C}}(\omega) = \begin{pmatrix} \omega - \epsilon_0 - \Sigma_{\mathrm{L}} - \Sigma_{\mathrm{R}} & -s \\ -s & \omega - f \end{pmatrix}^{-1}. \tag{A.4}$$

The quantum dot Green function is the (1, 1) term of the above matrix

$$G_{\mathrm{Dot}}(\omega) = \frac{\omega - f}{(\omega - \epsilon_0 - \Sigma_{\mathrm{L}} - \Sigma_{\mathrm{R}})(\omega - f) - s^2}. \tag{A.5}$$

Appendix B. Calculation of the self-energy

Consider semi-infinite periodic layers with an edge. We can divide the lead into layers and assume only the overlap between the nearest neighbours is nonzero. A quantum dot coupled to this lead only interacts with the surface layer of the lead. In the following, we will calculate the self-energy due to the coupling between the dot and the lead by the surface Green function instead of by simply assuming the wide-band limit.

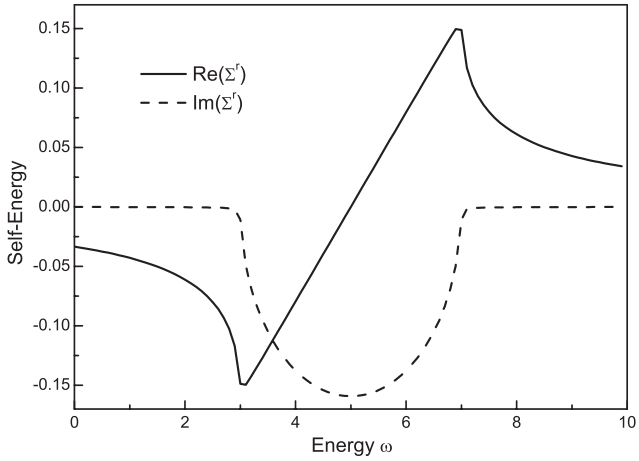

Figure B.1. Self-energy profile due to the coupling between the semi-infinite lead and the quantum dots.

In the one-dimensional tight-binding nearest-neighbour approximation, the Hamiltonian for the lead (equation (2)) is tridiagonal and can be written as

$$H = \begin{pmatrix} 0 & t & 0 & \cdots \\ t & 0 & t & \cdots \\ 0 & t & 0 & \ddots \\ \vdots & \vdots & \ddots & \ddots \end{pmatrix}. \tag{B.1}$$

The Green function of the lead can be obtained by

$$G = (\omega - H)^{-1} = \begin{pmatrix} G_{00} & G_{01} & G_{02} & \cdots \\ G_{10} & G_{11} & G_{12} & \cdots \\ G_{20} & G_{21} & G_{22} & \ddots \\ \vdots & \vdots & \ddots & \ddots \end{pmatrix}. \tag{B.2}$$

From equations (B.1) and (B.2) and assuming that $G_{n0} \to 0$ when $n \to \infty$, G_{00} can be iteratively solved by

$$G_{00} = \left.\frac{1}{\omega - \Sigma_i}\right|_{i\to\infty}, \tag{B.3}$$

where

$$\begin{aligned} \Sigma_{i+1} &= \Sigma_i + t_i(\omega - U_i)t_i \\ t_{i+1} &= t_i(\omega - U_i)^{-1}t_i \\ U_{i+1} &= U_i + 2t_i(\omega - U_i)^{-1}t_i. \end{aligned} \tag{B.4}$$

The initial values for t_0, U_0, and Σ_0 are

$$t_0 = t; \qquad \text{and} \qquad U_0 = \Sigma_0 = 0. \tag{B.5}$$

Then the self-energy due to coupling between the quantum dots and the lead can be written as

$$\Sigma(\omega) = H_{\mathrm{CL}} G_{00} H_{\mathrm{LC}}, \tag{B.6}$$

where H_{LC} and H_{CL} describe the tunnelling onto (off) the quantum dots from the lead. The retarded self-energy is calculated from $\Sigma^{\mathrm{r}}(\omega) = \Sigma(\omega + \mathrm{i}\delta)$, where δ is an infinitesimal positive number. The calculated self-energy profile is illustrated in figure B.1. The maximum of the imaginary part of Σ appears at the energy of the dot electron level, while the real part of Σ at that point is zero.

References

[1] Chen J, Reed M A, Rawlett A M and Tour J M 1999 *Science* **286** 1550
[2] Orellan P and Claro F 2003 *Phys. Rev. Lett.* **90** 178302
[3] Qin H, Holleitner A W, Eberl K and Blick R H 2001 *Phys. Rev.* B **64** 241302(R)
[4] Güçlü A D, Sun Q F and Guo H 2003 *Phys. Rev.* B **68** 245323
[5] Lambo S and Joshi S K 2000 *Phys. Rev.* B **62** 1580
[6] Kouwenhoven L and Marcus C 1998 *Phys. World* (June) 35
[7] Beenakker C and Schönenberger C 2003 *Phys. Today* (May) 37
[8] Imry Y and Landauer R 1999 *Rev. Mod. Phys.* **71** S306
[9] Meir Y and Wingreen N S 1992 *Phys. Rev. Lett.* **68** 2512
[10] Mozyrsky D, Fedichkin L, Gurvitz S A and Berman G P 2002 *Phys. Rev.* B **66** 161313
[11] Gurvitz S A, Fedichkin L, Mozyrsky D and Berman G P 2003 *Phys. Rev. Lett.* **91** 066801
[12] Chen L Y and Ting C S 1991 *Phys. Rev.* B **43** 4534
[13] Iannaccone G, Lombardi G, Macucci M and Pellegrini B 1998 *Phys. Rev. Lett.* **80** 1054
[14] Zhu J X and Balatsky A V 2003 *Phys. Rev.* B **67** 165326
[15] Blanter Y M and Büttiker M 2000 *Phys. Rep.* **336** 1
[16] Landauer R 1998 *Nature* **392** 658
[17] Xiao M, Martin I and Jiang H W 2003 *Phys. Rev. Lett.* **93** 93
[18] Büttiker M 1992 *Phys. Rev.* B **46** 12485
[19] Li Y P, Tsui D C, Heremans J J, Simmons J A and Weimann G W 1990 *Appl. Phys. Lett.* **57** 774
[20] Kumar A, Saminadayar L, Glattli D C, Jin Y and Etienne B 1996 *Phys. Rev. Lett.* **76** 2778
[21] Wei Y, Wang B G, Wang J and Guo H 1999 *Phys. Rev.* B **60** 16900
[22] Gurvitz S A 1998 *Phys. Rev.* B **57** 6602
[23] Dong B and Lei X L 2002 *J. Phys.: Condens. Matter* **14** 4963
[24] Deshpande M R, Sleight J M, Reed M A, Wheeler R G and Matyi R J 1996 *Phys. Rev. Lett.* **76** 1328
[25] Gryglas M, Baj M, Chenaud B, Jouault B, Cavanna A and Faini G 2004 *Phys. Rev.* B **69** 165302
[26] Wingreen N, Jacobsen K and Wilkins J 1989 *Phys. Rev.* B **40** 11834
[27] Lundin U and McKenzie R H 2002 *Phys. Rev.* B **66** 075303
[28] Mahan G D 1990 *Many-Particle Physics* 2nd edn (New York: Plenum)